Lattice-Fluid Theory Prediction of High-Density Polyethylene−Branched Polyolefin Blend Miscibility

Ioannis G. Economou*

Molecular Modelling of Materials Laboratory, Institute of Physical Chemistry, National Research Centre for Physical Sciences "Demokritos", GR-153 10 Aghia Paraskevi Attikis, Greece

Received September 30, 1999; Revised Manuscript Received February 18, 2000

ABSTRACT: Polyolefin blend miscibility is very important for a number of technological applications. Its experimental measurement is far from trivial and requires highly sophisticated expensive experimental techniques. In this work, the lattice-fluid theory of Sanchez and Lacombe is used to calculate the phase equilibria of binary polyolefin blends. The miscibility of high-density polyethylene with three branched polyolefins is computed as a function of polymer chain size and architecture, temperature, and pressure. The binary interaction parameter of the model is fitted to experimental data for the high-density polyethylene−poly(ethylene-*alt*-propylene) and used for all the blends examined. Lattice-fluid theory predictions are in qualitative agreement with limited experimental data available and with predictions from other theoretical models. The proposed relatively simple methodology can be used as a guideline to determine the phase behavior of polyolefin blends.

Introduction

Over the past 15 years, polymer blends have attracted considerable interest both in the research community and in industry. As a result, a better understanding and detailed description and prediction of the blend properties is necessary. One crucial issue is the miscibility of the polymers in a blend. For most applications, it is desirable that the phase behavior of the polymer blend be accurately known, since it will affect the physical properties and, consequently, the use of the blend for a specific application. In addition, the design of new polymeric materials for polymer blends with tailored properties is of great interest. This work focus on polyolefin blends, which is the most widely used and studied class of polymer blends.

Several experimental research groups have studied the phase behavior of polyolefin blends that differ in molecular architecture, polarity, molecular size, and composition using small-angle neutron scattering (SANS), small-angle X-ray scattering (SAXS), small-angle light scattering (SALS), and solid-state NMR. The pioneering work of Bates and co-workers[1−3] on the phase behavior of protonated and deuterated polyolefins indicated that a blend of a partially deuterated polyolefin with the corresponding protonated polyolefin exhibits an upper critical solution temperature (UCST) if the molecular weight (MW) is high enough. Subsequent work[4−22] provided more details on the effect of molecular architecture (degree of branchiness, etc.), temperature, pressure, and deuteration on the miscibility of many polymer blends of saturated polyolefins such as linear and branched polyethylene, poly(ethylene−propylene), polypropylene, polyisobutylene, and poly(ethylene-*co*-1-butene). Furthermore, it was shown that various polyolefin blends exhibit lower critical solution temperature (LCST) behavior, as for example poly(ethylene−propylene)−polyisobutylene[15] and head-to-head polypropylene−polyisobutylene.[23] Despite however the extensive effort by different research groups, the phase behavior of many common binary blends, as for example high-density polyethylene (HDPE)−low-density polyethylene (LDPE), is not fully understood, yet.[24−26] The difficulty in the interpretation of SANS data is mainly due to the similarity in the chemical structure of the constituent polymers (composed of methyl and methylene groups only). This problem can be partially resolved by the deuteration of one of the polymers.

From the modeling point of view, nonideal mixing of polyolefins has been modeled using various approaches. Graessley and co-workers used the Flory−Huggins expression for the Gibbs energy of mixing.[13,14] In this case, the χ parameter was estimated from the solubility parameters of the constituent polymers, which were fit to the experimental blend data.[10] Several qualitative trends were identified concerning the miscibility of hydrocarbon polymers, and some predictive rules were proposed.[11] Good agreement between experimental data and model correlation was obtained for most of the binary blends examined.

A more elaborate approach was proposed by Fredrickson and Bates[27−29] using conformational asymmetry theory for blends of almost athermal polyolefins (either homopolymers or copolymers). They developed theoretical guidelines for the polymer−polymer miscibility based on nonlocal properties of the polymers, namely the radius of gyration and molecular volume. The Graessley et al. approach seems to emphasize the energetic effects on the mixing of polymers whereas the Fredrickson et al. approach is based on the packing effects on the polymer miscibility.

Freed and Dudowicz[30,31] used the compressible lattice cluster theory (LCT) to study the effect of short branches on the miscibility of polymer blends. Their calculations revealed the relative effect of enthalpy and entropy on the miscibility of polyolefin blends and permitted the understanding of certain experimental trends.

Lattice Monte Carlo simulation has been used extensively for the study of polymer blends.[32,33] Simulation results provided some qualitative trends concerning the parameters that control miscibility of real polymer blends, such as the difference in the chain length of the

* Tel ++ 30 1 6503963; Fax ++ 30 1 6511766; e-mail economou@mistras.chem.demokritos.gr.

10.1021/ma991656j CCC: $19.00
Published on Web 06/01/2000

polymers and the energetic interactions between like and unlike chains. Off-lattice molecular simulation has been restricted so far to simple model systems. For example, Weinhold et al.[34] examined the effect of chain stiffness on the structure and thermodynamic properties of polymer blends with Monte Carlo simulation using a tangent hard-sphere intermolecular potential for the polymer chain and concluded that entropic effects alone cannot impose phase separation in hydrocarbon polymer blends; enthalpic effects are needed as well to explain limited miscibility phenomena. Stevenson et al.[35] examined the structure of athermal polymer blends with molecular dynamics, and results were in good agreement with calculations from the polymer reference interaction site model (PRISM). Gromov and de Pablo used a fully flexible Lennard-Jones chain model to study the structure, using hybrid Monte Carlo simulation,[36] and the phase equilibria, using expanded Gibbs ensemble Monte Carlo simulation,[37] of binary polymer blends and obtained good agreement with calculations based on the self-consistent PRISM. Furthermore, Kumar and Weinhold[38] calculated the phase equilibria of two different Lennard-Jones polymer blends where the polymers were different (a) in chain stiffness and (b) in Lennard-Jones energetic parameters. Semigrand ensemble Monte Carlo simulation indicated that in both cases immiscibility occurs. More recently, thermodynamic and structure properties of different polyolefins that control blend miscibility were calculated through molecular dynamics simulation.[39,40]

A microscopic model based on PRISM, which accounts for the chain architecture, and single chain Monte Carlo simulation was developed by Rajasekaran et al.[41] and was used to predict the phase behavior of polyethylene−*i*-polypropylene. The blend was found to be highly immiscible with a very high UCST value.

Semiempirical equations of state (EoS) such as the Flory−Orwoll−Vrij EoS,[42−45] the lattice-fluid theory of Sanchez and Lacombe,[45−47] the Patterson EoS,[46] the Born−Green−Yvon (BGY) lattice model,[23] and others have been used successfully for the correlation and prediction of the phase equilibria of binary polymer blends containing polyolefins (either homopolymers or copolymers) and other polymers (such as polystyrene, poly(vinyl methyl ether), etc.).

In this work, the lattice-fluid theory (LFT) of Sanchez and Lacombe[48,49] is used to calculate the phase equilibria of binary polymer blends of HDPE with branched polyolefins of different architecture. The branched polyolefins examined are poly(ethylene-*alt*-propylene) (PEP), *i*-polypropylene (iPP), and *i*-poly(1-butene) (iPB). All three polymers consist of small branches (either methyl or ethyl groups). A binary interaction parameter is fitted to the experimental UCST for HDPE−PEP.[50] A systematic investigation of the effect of chain architecture, polymer MW, and pressure on the binodal and spinodal curves and critical point is presented. It is shown that LFT predictions are in qualitative agreement with limited experimental data available for the blends examined. Furthermore, it can be used as a guide for the design of miscible polyolefin blends.

Theory and Computational Details

LFT is a lattice model developed for the calculation of thermodynamic properties of small molecules and polymers.[48,49] According to LFT, every molecule of the fluid (either pure component or mixture) occupies r sites in the lattice. At the same time, the lattice contains N_0 vacant sites (holes) that change as a function of the state of the fluid (gaseous or liquid), temperature, and pressure. In this way, LFT is able to account explicitly for the free volume effects which are very important in high-pressure polymer phase equilibria, unlike earlier incompressible lattice models (such as the Flory−Huggins model[51]). The LFT EoS is given from the expression

$$\tilde{\rho}^2 + \tilde{P} + \tilde{T}\left[\ln(1-\tilde{\rho}) + \left(1 - \frac{1}{r}\right)\tilde{\rho}\right] = 0 \qquad (1)$$

where $\tilde{\rho}$ ($\equiv\rho/\rho^*$), $\tilde{P}$ ($\equiv P/P^*$), and $\tilde{T}$ ($\equiv T/T^*$) are the reduced density, reduced pressure, and reduced temperature, respectively. The LFT is a three-parameter EoS. These parameters are the characteristic temperature, T^*, the characteristic pressure, P^*, and the characteristic density, ρ^*. In the case of polymers, the parameters are calculated by fitting the EoS to melt densities over a wide temperature and pressure (usually from 0 to 2000 bar) range. The parameters for the polymers examined in this work were obtained from the literature[52,53] and are shown in Table 1. Parameter r is calculated from the expression

Table 1. LFT Parameters for the Polymers Examined in This Work

polymer	T^* (K)	P^* (bar)	ρ^* (g/cm^3)
HDPE[a]	615.0	3662	0.9137
PEP[b]	611.9	4453	0.9242
IPP[a]	633.0	3664	0.9126
IPB[a]	609.0	3775	0.9312

[a] From ref 52. [b] From ref 53.

$$r = \frac{MP^*}{RT^*\rho^*} \qquad (2)$$

where M is the MW. Equation 1 is generalized to mixtures with the use of appropriate mixing rules. In this work, the mixing rules proposed by Lacombe and Sanchez[49] for the LFT are used. Every component i in the mixture is characterized by the parameters are T_i^*, P_i^*, ρ_i^*, v_i^* ($=RT_i^*/P_i^*$), and r_i^0 ($=M_i/\rho_i^* v_i^*$). Two different volume fractions are defined according to the expressions

$$\varphi_i^0 = \frac{m_i/\rho_i^* v_i^*}{\sum_i m_i/\rho_i^* v_i^*} \qquad (3)$$

$$\varphi_i = \frac{m_i/\rho_i^*}{\sum_i m_i/\rho_i^*} \qquad (4)$$

where m_i is the weight fraction of i, and the summation is over all the components. Throughout this paper, when we refer to the volume fraction, we refer to φ_i. The number of sites occupied by molecule i in the lattice of the mixture is calculated from the expression

$$r_i = r_i^0 \frac{\varphi_i}{\varphi_i^0} \qquad (5)$$

The characteristic parameters of the mixture are cal-

culated from the expressions

$$T^* = \sum_i \sum_j \varphi_i \varphi_j T^*_{ij}, \quad T^*_{ij} = \sqrt{T^*_i T^*_j}\zeta_{ij} \tag{6}$$

$$v^* = \sum_i \varphi^0_i v^*_i \tag{7}$$

$$\rho^* = \frac{1}{\sum_i m_i/\rho^*_i} \tag{8}$$

$$P^* = RT^*/v^* \tag{9}$$

$$\frac{1}{r} = \sum_i \frac{\varphi_i}{r_i} = \sum_i \frac{\varphi^0_i}{r^0_i} \tag{10}$$

In eq 6, ζ_{ij} is a binary interaction parameter between species i and j and usually is fitted to experimental data for the specific binary mixture. For hydrocarbon mixtures, ζ_{ij} is close to unity.[49]

In the case of a binary mixture, the chemical potential of component i is calculated from the expression (j is the second component):

$$\frac{\mu_i}{RT} = \ln \varphi_i + \left(1 - \frac{r_i}{r_j}\right)\varphi_j + r^0_i\tilde{\rho}\left[\chi_{ij} + \left(1 - \frac{v^*_i}{v^*_j}\right)\lambda_{ij}\right]\varphi^2_j + r^0_i T^*_i \frac{\tilde{P}_i/\tilde{\rho} - \tilde{\rho}}{T} + r^0_i\left[\left(\frac{1}{\tilde{\rho}} - 1\right)\ln(1 - \tilde{\rho})\right] + \ln \tilde{\rho} \tag{11}$$

where χ_{ij} and λ_{ij} are defined as

$$\chi_{ij} = \frac{T^*_i + T^*_j - 2T^*_{ij}}{T} \tag{12}$$

$$\lambda_{ij} = \frac{T^*_i - T^*_j}{T} + (\varphi_i - \varphi_j)\chi_{ij} = -\lambda_{ji} \tag{13}$$

In this work, the binodal (coexistence curve) and the spinodal of binary polymer blends are calculated. The binodal is calculated by equating the chemical potential of the two polymers (1 and 2) in each of the two phases (I and II):

$$\mu^{\mathrm{I}}_1(T,P,\varphi^{\mathrm{I}}_1) = \mu^{\mathrm{II}}_1(T,P,\varphi^{\mathrm{II}}_1)$$

$$\mu^{\mathrm{I}}_2(T,P,\varphi^{\mathrm{I}}_2) + \mu^{\mathrm{II}}_2(T,P,\varphi^{\mathrm{II}}_2) \tag{14}$$

whereas the spinodal is calculated from the equation

$$\left(\frac{\partial \mu_1(T,P,\varphi_1)}{\partial \varphi_1}\right)_{T,P} = 0 \tag{15}$$

The mixture critical point corresponds to the contact of binodal and spinodal curves and mathematically is calculated from the expression

$$\left(\frac{\partial^2 \mu_1(T,P,\varphi_1)}{(\partial \varphi_1)^2}\right)_{T,P} = 0 \tag{16}$$

Results and Discussion

Maurer et al.[50] used SANS measurements in order to determine the spinodal and cloud point curves of the HDPE−PEP binary polymer blend. The MW and the polydispersity index of the two almost monodisperse polymers were 22 000 and 1.05 for HDPE and 23 000 and 1.03 for PEP, respectively. The critical temperature (UCST) of this blend was estimated to be 407 ± 5 K. The LFT binary interaction parameter, ζ_{ij}, was fitted to the critical temperature and used subsequently for the calculation of the binodal and spinodal curves. The resulted value ($\zeta_{ij} = 0.999\ 15$) is consistent with the fact that HDPE and PEP are composed of chemically similar groups (CH_3, CH_2, and CH), and so ζ_{ij} should be close to unity. In all calculations throughout this paper, the polymers are considered to be monodisperse. In Figure 1, experimental data and model predictions are presented. LFT predicts a lower HDPE volume fraction at the critical point. Furthermore, the calculated coexistence curve in the vicinity of the critical point is narrower than the experimental data suggest. This is a typical behavior for a mean-field model such as LFT. Predictions from the BGY model which accounts for the local interactions are in better agreement with the experimental data concerning the critical composition.[23] However, the shape of the phase envelope in the critical region is similar to LFT (Figure 2 of ref 23). Conclusively, the overall agreement between LFT prediction and experimental data is satisfactory, considering also the statistical uncertainty in the measurements.

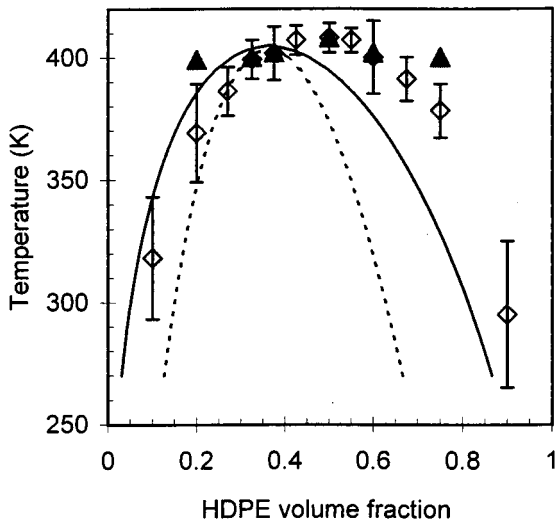

Figure 1. Phase diagram of $HDPE_{22\,000}$−$PEP_{23\,000}$ blend as a function of the HDPE volume fraction. Experimental cloud points (solid triangles) and spinodal temperatures (open diamonds).[50] LFT calculations are shown as solid lines (binodal curve) and dashed lines (spinodal curve).

The effect of polymer MW on the phase behavior of the HDPE−PEP blend is shown in Figure 2 where calculations are presented for blends of $HDPE_{22\,000}$ (subscripts indicate the MW) with $PEP_{23\,000}$, $PEP_{70\,000}$, and $PEP_{150\,000}$. For each blend, the thick curve corresponds to the binodal and the thin curve to the spinodal. As the MW of one of the polymers increases, miscibility decreases. Mutual solubilities (volume fractions) decrease whereas the critical temperature increases. In Figures 3 and 4, the variation of the blend critical temperature and critical composition (in terms of HDPE volume fraction) as a function of the PEP MW is shown. The MW of HDPE is 22 000 in all cases. For low PEP MW values (below approximately 8000) the two polymers are completely miscible. As the PEP MW increases up to approximately 80 000−100 000, the critical tem-

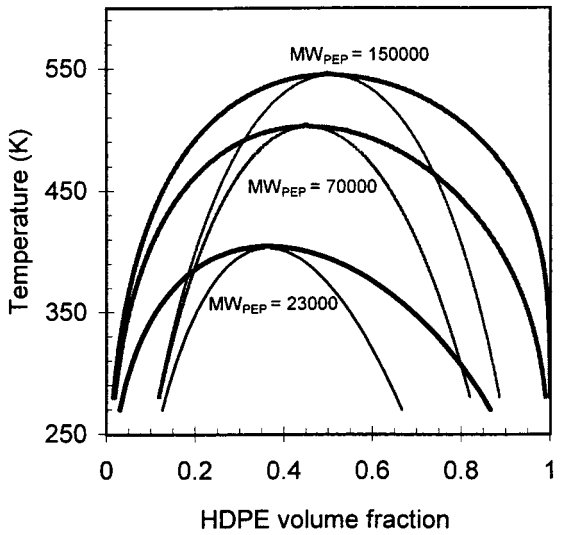

Figure 2. LFT predictions of the binodal curve (thick lines) and spinodal curve (thin lines) of $HDPE_{22\,000}$−$PEP_{23\,000}$, $HDPE_{22\,000}$−$PEP_{70\,000}$, and $HDPE_{22\,000}$−$PEP_{150\,000}$ blends as a function of the HDPE volume fraction.

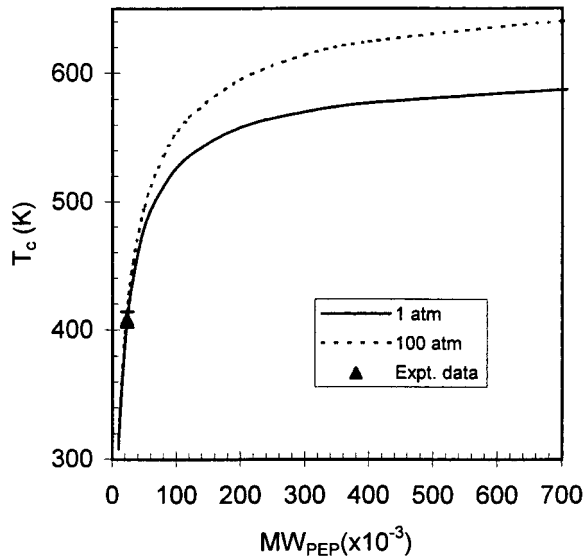

Figure 3. LFT predictions of the critical temperature of binary $HDPE_{22\,000}$ blends with PEP of different MW as a function of PEP MW at 1 and 100 atm. The experimental point for $PEP_{23\,000}$ at 1 atm is from ref 50.

perature and critical composition increase sharply. For higher PEP MW values, the change is much smaller. This indicates that the polymer molecular size has a strong effect on the blend miscibility for small and intermediate values and a much smaller effect for higher values. Such behavior agrees with predictions from the BGY lattice model.[23]

In Figures 3 and 4, LFT predictions are shown for two different pressures, 1 and 100 atm. Interestingly, the critical temperature increases with an increase in pressure for all molecular weight values, and so pressure makes these polymers less miscible. This is also evident from Figure 5 where the variation of critical temperature with pressure is shown for the blend $HDPE_{22\,000}$−$PEP_{23\,000}$. From the physical point of view, LFT predicts that as pressure (and consequently density) increases, like polymer chains achieve better packing by excluding unlike chains. This behavior is consistent with experimental data for polyolefin blends.[20]

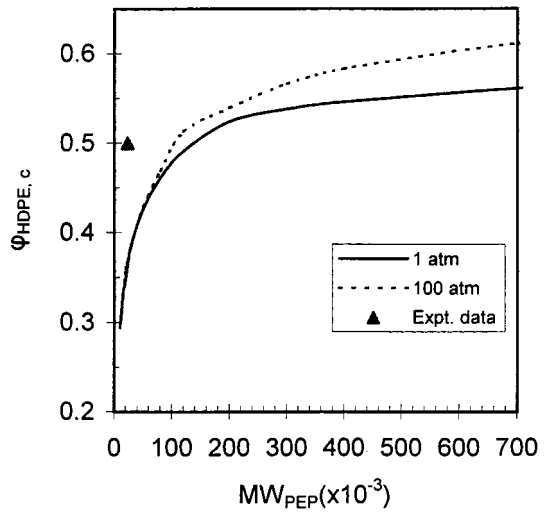

Figure 4. LFT predictions of the HDPE volume fraction ($\varphi_{HDPE,c}$) at the blend critical temperature of binary $HDPE_{22,000}$ blends with PEP of different MW as a function of PEP MW, at 1 and 100 atm. The experimental point for $PEP_{23\,000}$ at 1 atm is from ref 50.

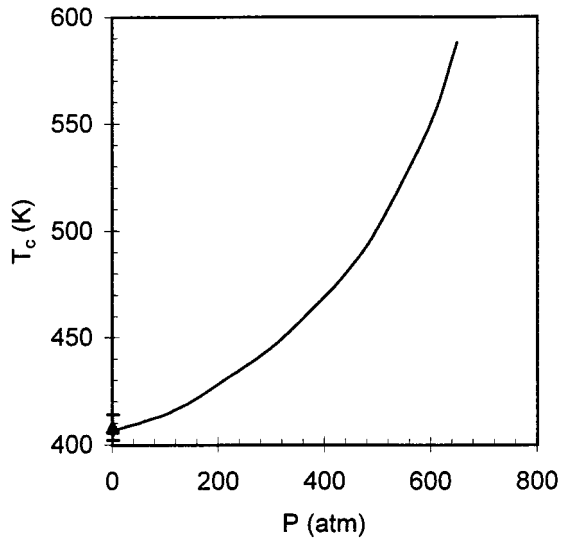

Figure 5. LFT predictions of the critical temperature of $HDPE_{22\,000}$−$PEP_{23\,000}$ blend as a function of pressure. The experimental point at 1 atm is from ref 50.

As Rabeony et al.[20] explain, for mixtures exhibiting UCST behavior, the mixed state is favored by heating, i.e., by lowering the density of the mixture. The pressure increase has the opposite effect, and so miscibility decreases. The LCT[29] and BGY lattice model[23] predict a similar pressure effect for HDPE−PEP.

Another binary blend examined in this work is HDPE−iPP. iPP polymer chains are composed of the same groups as the PEP chains, and so it is assumed that the binary interaction parameter, ζ_{ij}, remains unchanged. This approximation was shown to be very good for the case of low MW hydrocarbon mixtures.[49] In Figure 6, LFT binodal and spinodal curves are shown for the binary blends: $HDPE_{22\,000}$−$iPP_{23\,000}$, $HDPE_{22\,000}$−$iPP_{70\,000}$, and $HDPE_{22\,000}$−$iPP_{150\,000}$. Similarly to the first blend examined (HDPE−PEP), the increase in the MW of one of the polymers increases the immiscibility. As its branch content increases, from 25 short branches per 100 backbone carbon atoms for PEP to 50 short branches per 100 backbone carbon atoms for iPP, the miscibility of the branched polyolefin with HDPE decreases. For

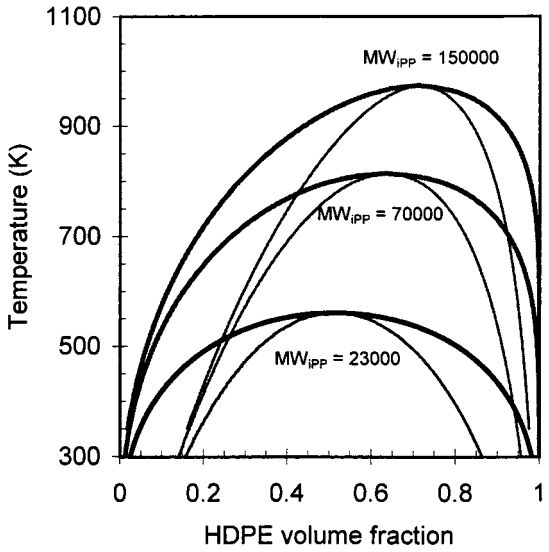

Figure 6. LFT predictions of the binodal curve (thick lines) and spinodal curve (thin lines) of $HDPE_{22\,000}$−$iPP_{23\,000}$, $HDPE_{22\,000}$−$iPP_{70\,000}$, and $HDPE_{22\,000}$−$iPP_{150\,000}$ blends as a function of the HDPE volume fraction.

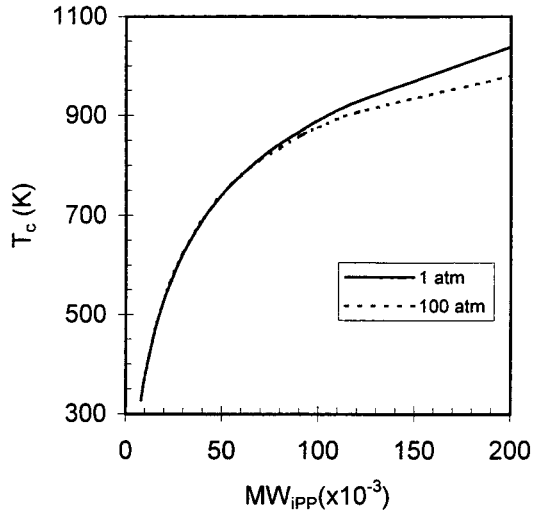

Figure 7. LFT predictions of the critical temperature of binary $HDPE_{22\,000}$ blends with iPP of different MW as a function of iPP MW at 1 and 100 atm.

example, the critical temperature for $HDPE_{22\,000}$−$PEP_{23\,000}$ is 404 K and for $HDPE_{22\,000}$−$iPP_{23\,000}$ is 562 K. This behavior holds for the entire range of branched polyolefin MW examined and is a clear indication of the chain architecture effect on the blend phase behavior. Calculations presented here are in qualitative agreement with previous LCT[30] and PRISM[41] predictions. However, the PRISM[41] UCST is much higher than the UCST presented here. Although no clear conclusions can be made, the origin for this difference can be the local correlations in the blend that PRISM calculates explicitly. Of course, the high-temperature calculations are only theoretical predictions. Polymer chains become progressively unstable above approximately 550 K. Such thermal chain destruction is not accounted by an equilibrium thermodynamic model such as LFT.

In Figure 7, the effect of iPP MW on the blend critical temperature is shown for two different pressures. The pressure effect is, in general, small and becomes appreciable only above a MW value of approximately 75 000. Interestingly, for iPP MW values higher than

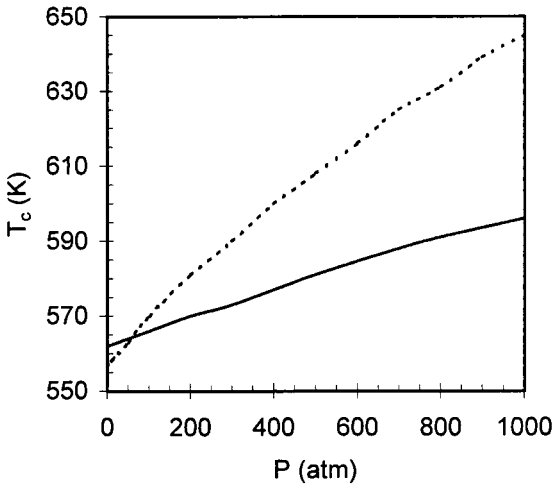

Figure 8. LFT predictions of the critical temperature of $HDPE_{22\,000}$−$iPP_{23\,000}$ blend (solid line) and $HDPE_{22\,000}$−$iPB_{23\,000}$ blend (dashed line) as a function of pressure.

60 000, the critical temperature decreases with pressure, and so pressure induces miscibility between HDPE and iPP. It is certain that additional experimental measurements are needed in order to verify whether this pressure effect is realistic. Finally, in Figure 8 the pressure effect on the critical temperature for the blend $HDPE_{22\,000}$−$iPP_{23\,000}$ is shown (solid line). Clearly, pressure has a much smaller effect for this blend compared to the $HDPE_{22\,000}$−$PEP_{23\,000}$ blend (Figure 5). To a great extent, this should be attributed to the similar values for P^* and ρ^* that HDPE and iPP have compared to HDPE and PEP (Table 1). This similarity reflects the fact that the compressibility of iPP is closer to the compressibility of HDPE than the compressibility of PEP, as predicted by the LFT in the pressure range examined here. A detailed discussion of the EoS parameter effects on the miscibility of polyolefin blends can be found in ref 43.

The third binary blend examined here is HDPE−iPB. In this case, the number of branches per 100 backbone carbon atoms remains unchanged compared to iPP, but the branch size increases from methyl (CH_3) to ethyl (C_2H_5). In Figure 9, LFT calculations are shown for the binodal and spinodal curves of the binary blends: $HDPE_{22\,000}$−$iPB_{23\,000}$, $HDPE_{22\,000}$−$iPB_{70\,000}$, and $HDPE_{22\,000}$−$iPB_{150\,000}$. (ζ_{ij} was set again equal to 0.999 15.) The branched polyolefin MW has a similar effect on the phase behavior of this blend as on the other two blends examined. The phase diagram for $HDPE_{22\,000}$−$iPB_{23\,000}$ is similar to the phase diagram for $HDPE_{22\,000}$−$iPP_{23\,000}$ whereas the other two blends with a higher iPB MW (70 000 and 150 000) exhibit lower critical temperature compared to the corresponding iPP blends of Figure 6. In Figure 10, the iPB MW effect on the critical temperature is shown for two different pressures. In this case, pressure increases immiscibility over the entire MW range. Finally, in Figure 8 the pressure effect on the critical temperature of $HDPE_{22\,000}$−$iPB_{23\,000}$ is shown (dashed line).

The LFT calculations presented in this work reveal that the increase in the branch number density (from PEP to iPP) has a much pronounced effect than the increase in the branch size (from methyl in the case of iPP to ethyl in the case of iPB) on the phase diagram of HDPE with a branched polyolefin.

Finally, LFT calculations agree well with predictions based on the conformational asymmetry theory of Fre-

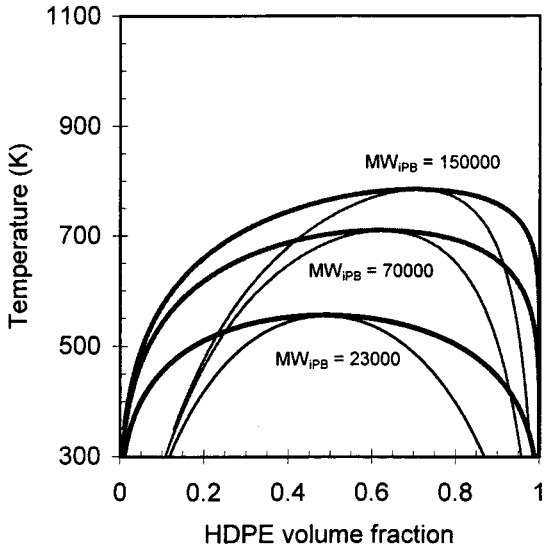

Figure 9. LFT predictions of the binodal curve (thick lines) and spinodal curve (thin lines) of $HDPE_{22\,000}$−$iPB_{23\,000}$, $HDPE_{22\,000}$−$iPB_{70\,000}$, and $HDPE_{22\,000}$−$iPB_{150\,000}$ blends as a function of the HDPE volume fraction.

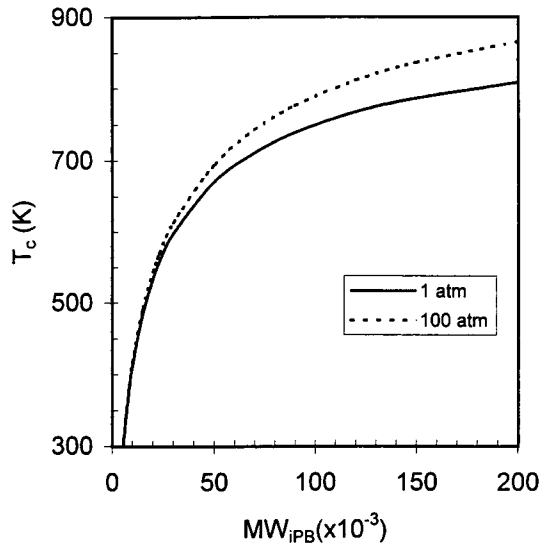

Figure 10. LFT predictions of the critical temperature of binary $HDPE_{22\,000}$ blends with iPB of different MW as a function of iPB MW at 1 and 100 atm.

drickson and Bates.[28] According to that theory, the miscibility of athermal binary blends of linear homopolymers A and B is controlled by the conformational asymmetry ratio ϵ defined as

$$\epsilon \equiv \left(\frac{\beta_A}{\beta_B}\right)^2 = \frac{R_A^2/V_A}{R_B^2/V_B} \qquad (17)$$

where R_i^2 and V_i are the mean-squared radius of gyration and molecular volume of species i, respectively. In order that a polymer blend is miscible, ϵ should be close to unity. To a good approximation, all of the polymers examined here are linear homopolymers that mix almost athermally. The conformational asymmetry ratios at ambient conditions for the three blends examined in this work are $\epsilon_{HDPE-PEP} \sim 1.8$,[13,45,53,54] $\epsilon_{HDPE-iPP} \sim 2.1$,[45,54] and $\epsilon_{HDPE-iPB} \sim 3.1$.[45,54,55] As a result, conformational asymmetry theory predicts that all three blends are immiscible. Furthermore, immiscibility increases for the blends of HDPE with iPP and with iPB compared to the HDPE−PEP blend, in accordance with LFT predictions. On the other hand, if one treats the branched polyolefins as branched homopolymers, then conformational asymmetry theory predicts that the nonideality of a blend of chemically similar linear and branched homopolymers increases as the branch points on each branched macromolecule increase.[28] This, again, is in accordance with the LFT predictions presented above. It should be mentioned here that the conformational asymmetry theory for branched homopolymers was developed assuming Gaussian statistics for the backbone and the branches. This assumption of course is not realistic for the case of short branches examined here, and so the treatment of branched polyolefins as linear homopolymers is more appropriate within the context of conformational asymmetry theory.

Conclusions

In this work, LFT was used to calculate the phase equilibria of binary blends of HDPE with three branched polyolefins of variable MW. The effect of polymer chain size and architecture, temperature, and pressure was identified. The limited experimental data available for $HDPE_{22\,000}$−$PEP_{23\,000}$ were used to evaluate the binary interaction parameter used throughout the calculations. The methodology presented here can be applied to other types of polyolefins blends (as, for example, branched polyolefins of different architecture) as well as to LCST phase equilibria. Preliminary calculations are encouraging and will be the subject of a future communication.

It should be made clear that LFT accounts for the chain architecture implicitly through the pure component parameters which are fitted to experimental *PVT* data. Furthermore, local interactions between unlike chains are calculated through the binary interaction parameter ζ_{ij}. Because of the limited experimental data available, it was assumed here that ζ_{ij} is the same for all of the mixtures examined. Although this is a very good approximation for the case of mixtures of low MW hydrocarbons (*n*-alkanes, branched alkanes, etc.), it becomes less accurate as the MW of the components increases. It is well-known that equation-of-state predictions for polymer solutions and blends are very sensitive to the binary interaction parameter.[16,56] It is difficult to make an estimation of the error that such approximations introduce into the predictions presented here. Additional experimental data are required in order to test some of these assumptions and the subsequent model predictions.

Despite these limitations, the relatively simple method presented here can be used as a guideline for the estimation of polyolefin blend miscibility. It offers a significant advantage over other widely used lattice models such as the solubility parameter approach of Graessley and co-workers:[11,13,14] It accounts explicitly for the energetic interactions between unlike molecules and for the compressibility (free-volume) effects which control blend miscibility as pressure changes. It can be combined with the accurate but relatively expensive experimental techniques available in order to develop a better methodology for the estimation of the model parameters. In this way, the binary interaction parameter, ζ_{ij}, can be temperature or MW dependent, and even an additional binary parameter can be added (in the mixing rule for the characteristic volume, eq 7, for example). This approach can lead to a powerful predictive model.

Acknowledgment. Dr. David J. Lohse is gratefully acknowledged for providing his data and manuscript prior to publication. Stimulating discussions and suggestions by Professor Doros N. Theodorou are deeply appreciated. I am thankful to one of the referees for bringing ref 41 to my attention. This work was supported financially by the Greek General Secretariat of Research and Technology in the framework of the PABE program.

References and Notes

(1) Bates, F. S.; Wignall, G. D.; Koehler, W. C. *Phys. Rev. Lett.* **1985**, *55*, 2425−2428.
(2) Bates, F. S.; Wiltzius, P. *J. Chem. Phys.* **1989**, *91*, 3258−3274.
(3) Bates, F. S. *Science* **1991**, *251*, 898−905.
(4) Hill, M. J.; Barham, P. J.; Keller, A.; Rosney, C. C. A. *Polymer* **1991**, *32*, 1384−1393.
(5) Balsara, N. P.; Fetters, L. J.; Hadjichristidis, N.; Lohse, D. J.; Han, C. C.; Graessley, W. W.; Krishnamoorti, R. *Macromolecules* **1992**, *25*, 6137−6147.
(6) Gehlsen, M. D.; Rosedale, J. H.; Bates, F. S.; Wignall, G. D.; Hansen, L.; Almdal, K. *Phys. Rev. Lett.* **1992**, *68*, 2452−2455.
(7) Jinnai, H.; Hasegawa, H.; Hashimoto, T.; Han, C. C. *J. Chem. Phys.* **1993**, *99*, 4845−4854.
(8) Rhee, J.; Crist, B. *J. Chem. Phys.* **1993**, *98*, 4174−4182.
(9) Graessley, W. W.; Krishnamoorti, R.; Balsara, N. P.; Butera, R. J.; Fetters, L. J.; Lohse, D. J.; Schulz, D. N.; Sissano, J. A. *Macromolecules* **1994**, *27*, 3896−3901.
(10) Graessley, W. W.; Krishnamoorti, R.; Balsara, N. P.; Fetters, L. J.; Lohse, D. J.; Schulz, D. N.; Sissano, J. A. *Macromolecules* **1994**, *27*, 2574−2579.
(11) Graessley, W. W.; Krishnamoorti, R.; Reichart, G. C.; Balsara, N. P.; Fetters, L. J.; Lohse, D. J. *Macromolecules* **1995**, *28*, 1260−1270.
(12) Hill, M. J.; Barham, P. J. *Polymer* **1995**, *36*, 1523−1530.
(13) Krishnamoorti, R.; Graessley, W. W.; Balsara, N. P.; Lohse, D. J. *Macromolecules* **1994**, *27*, 3073−3081.
(14) Krishnamoorti, R.; Graessley, W. W.; Balsara, N. P.; Lohse, D. J. *J. Chem. Phys.* **1994**, *100*, 3894−3904.
(15) Krishnamoorti, R.; Graessley, W. W.; Fetters, L. J.; Garner, R. T.; Lohse, D. J. *Macromolecules* **1995**, *28*, 1252−1259.
(16) Krishnamoorti, R.; Graessley, W. W.; Dee, G. T.; Walsh, D. J.; Fetters, L. J.; Lohse, D. J. *Macromolecules* **1996**, *29*, 367−376.
(17) Lin, C. C.; Jeon, H. S.; Balsara, N. P.; Hammouda, B. *J. Chem. Phys.* **1995**, *103*, 1957−1971.
(18) Alamo, R. G.; Graessley, W. W.; Krishnamoorti, R.; Lohse, D. J.; Londono, J. D.; Mandelkern, L.; Stehling, F. C.; Wignall, G. D. *Macromolecules* **1997**, *30*, 561−566.
(19) Hammouda, B.; Balsara, N. P.; Lefebvre, A. A. *Macromolecules* **1997**, *30*, 5572−5574.
(20) Rabeony, M.; Lohse, D. J.; Garner, R. T.; Han, S. J.; Graessley, W. W.; Migler, K. B. *Macromolecules* **1998**, *31*, 6511−6514.
(21) White, J. L.; Brant, P. *Macromolecules* **1998**, *31*, 5424−5429.
(22) Seki, M.; Nakano, H.; Yamauchi, S.; Suzuki, J.; Matsushita, Y. *Macromolecules* **1999**, *32*, 3227−3234.
(23) Luettmer-Strathmann, J.; Lipson, J. E. G. *Macromolecules* **1999**, *32*, 1093−1102.
(24) Puig, C. C.; Odell, J. A.; Hill, M. J.; Barham, P. J.; Folkes, M. J. *Polymer* **1994**, *35*, 2452−2457.
(25) Schipp, C.; Hill, M. J.; Barham, P. J.; Cloke, V. M.; Higgins, J. S.; Oiarzabal, L. *Polymer* **1996**, *37*, 2291−2297.
(26) Agamalian, M.; Alamo, R. G.; Kim, M. H.; Londono, J. D.; Mandelkern, L.; Wignall, G. D. *Macromolecules* **1999**, *32*, 3093−3096.
(27) Bates, F. S.; Fredrickson, G. H. *Macromolecules* **1994**, *27*, 1065−1067.
(28) Fredrickson, G. H.; Liu, A. J.; Bates, F. S. *Macromolecules* **1994**, *27*, 2503−2511.
(29) Fredrickson, G. H.; Liu, A. J. *J. Polym. Sci., Polym. Phys.* **1995**, *33*, 1203−1212.
(30) Freed, K. F.; Dudowicz, J. *Macromolecules* **1996**, *29*, 625−636.
(31) Freed, K. F.; Dudowicz, J. *Macromolecules* **1998**, *31*, 6681−6690.
(32) Binder, K. In *Computer Simulation of Polymers*, Colbourn, E. A., Ed.; Longman Group: Harlow, UK, 1994.
(33) Müller, M.; Binder, K. *Macromolecules* **1995**, *28*, 1825−1834.
(34) Weinhold, J. D.; Kumar, S. K.; Singh, C.; Schweizer, K. S. *J. Chem. Phys.* **1995**, *103*, 9460−9473.
(35) Stevenson, C. S.; Curro, J. G.; McCoy, J. D.; Plimpton, S. J. *J. Chem. Phys.* **1995**, *103*, 1208−1215.
(36) Gromov, D. G.; de Pablo, J. J. *J. Chem. Phys.* **1995**, *103*, 8247−8256.
(37) Gromov, D. G.; de Pablo, J. J. *J. Chem. Phys.* **1998**, *109*, 10042−10052.
(38) Kumar, S. K.; Weinhold, J. D. *Phys. Rev. Lett.* **1996**, *77*, 1512−1515.
(39) Maranas, J. K.; Mondello, M.; Grest, G. S.; Kumar, S. K.; Debenedetti, P. G.; Graessley, W. W. *Macromolecules* **1998**, *31*, 6991−6997.
(40) Maranas, J. K.; Kumar, S. K.; Debenedetti, P. G.; Graessley, W. W.; Mondello, M.; Grest, G. S. *Macromolecules* **1998**, *31*, 6998−7002.
(41) Rajasekaran, J. J.; Curro, J. G.; Honeycutt, J. D. *Macromolecules* **1995**, *28*, 6843−6853.
(42) Walsh, D. J.; Dee, G. T.; Halary, J. L.; Ubiche, J. M.; Millequant, M.; Lesec, J.; Monnerie, L. *Macromolecules* **1989**, *22*, 3395−3399.
(43) Walsh, D. J.; Graessley, W. W.; Datta, S.; Lohse, D. J.; Fetters, L. J. *Macromolecules* **1992**, *25*, 5236−5240.
(44) Maier, R.-D.; Thomann, R.; Kressler, J.; Mülhaupt, R.; Rudolf, B. *J. Polym. Sci., Polym. Phys.* **1997**, *35*, 1135−1144.
(45) Han, S. J.; Lohse, D. J.; Condo, P. D.; Sperling, L. H. *J. Polym. Sci., Polym. Phys.* **1999**, *37*, 2835−2844.
(46) Rudolf, B.; Cantow, H. J. *Macromolecules* **1995**, *28*, 6586−6594.
(47) An, L.; Horst, R.; Wolf, B. A. *J. Chem. Phys.* **1997**, *107*, 2597−2602.
(48) Sanchez, I. C.; Lacombe, R. H. *J. Phys. Chem.* **1976**, *80*, 2352−2362.
(49) Lacombe, R. H.; Sanchez, I. C. *J. Phys. Chem.* **1976**, *80*, 2568−2580.
(50) Maurer, W. W.; Bates, F. S.; Lodge, T. P.; Almdal, K.; Mortensen, K.; Fredrickson, G. H. *J. Chem. Phys.* **1998**, *108*, 2989−3000.
(51) Flory, P. J. *Principles of Polymer Chemistry;* Cornell University Press: Ithaca, NY, 1953.
(52) Rodgers, P. A. *J. Appl. Polym. Sci.* **1993**, *48*, 1061−1080.
(53) Chen, S. J.; Chiew, Y. C.; Gardecki, J. A.; Nilsen, S.; Radosz, M. *J. Polym. Sci., Polym. Phys.* **1994**, *32*, 1791−1798.
(54) Zirkel, A.; Urban, V.; Richter, D.; Fetters, L. J.; Huang, J. S.; Kampmann, R.; Hadjichristidis, N. *Macromolecules* **1992**, *25*, 6148−6155.
(55) Hattam, P.; Gauntlett, S.; Mays, J. W.; Hadjichristidis, N.; Young, R. N.; Fetters, L. J. *Macromolecules* **1991**, *24*, 6199−6209.
(56) Liu, D. D.; Prausnitz, J. M. *Macromolecules* **1979**, *12*, 454−458.

MA991656J